PHYSICAL REVIEW A VOLUME 15, NUMBER 1 JANUARY 1977

Radiative decays of the $n = 2$ states of He-like ions

C. D. Lin,* W. R. Johnson,† and A. Dalgarno*
Center for Astrophysics, Harvard College Observatory and Smithsonian Astrophysical Observatory, Cambridge, Massachusetts 02138
(Received 19 July 1976)

The relativistic random-phase approximation (RRPA) is applied to study radiative transitions from $n = 2$ states along the He isoelectronic sequence. The strengths of various decay modes and the energy splittings of the $n = 2$ multiplets are investigated. At low Z the present results agree with earlier nonrelativistic studies, whereas, at high Z our results provide new information about oscillator strengths, branching ratios, and multiplet structure for the $n = 2$ states.

I. INTRODUCTION

Radiative transitions from the $n=2$ levels of He-like ions have been measured in solar spectra[1] and in the laboratory[2] for ions with nuclear charges Z ranging from 2 to 36. An $n=2$ level may decay to the ground state or to energetically lower $n=2$ states by emitting one or more photons.[3] Except for $2\,^1P_1$, the $n=2$ transitions to the ground state are all highly retarded because of angular momentum and parity restrictions. By contrast, transitions among the $n=2$ levels are often allowed by $E1$ selection rules.

Forbidden transitions to the ground state depend on high powers of the energy separation and consequently grow rapidly with Z. Thus transitions to the ground state dominate the decay scheme at high Z. At low Z, the allowed $E1$ transitions between $n=2$ levels tend to dominate the decay.

In this paper we examine in detail the variation in strength of the decay modes of the different $n=2$ levels along the entire isoelectronic sequence. Our study is carried out using relativistic techniques so that the entire range of ions can be considered. For low Z the present study agrees with existing accurate nonrelativistic calculations. We expect our results to be accurate at very high Z as well since the important relativistic effects are included in our formulation.

Energy splittings among the $n=2$ levels are crucial for the decay schemes and decay rates. We examine the complicated pattern of splittings along the sequence which is caused by the changing magnitudes of the electron-electron correlation and the Breit interaction, together with the fact that the $1s_{1/2}2s_{1/2}$ and $1s_{1/2}2p_{1/2}$ levels are degenerate at high Z and the $1s_{1/2}2p_{1/2}$ and $1s_{1/2}2p_{3/2}$ levels are degenerate at low Z.

In Sec. II we outline the RRPA method used in the present calculation. A comparison of the strengths of the decay modes from the various $n=2$ levels is given in Sec. III, and the energy splitting of the $n=2$ complex is considered in Sec. IV.

II. RRPA METHOD

The nonrelativistic random-phase approximation (RPA) has been applied successfully over the past few years to study various atomic properties. These nonrelativistic studies have established that the RPA gives a simple and accurate method for determining oscillator strengths for allowed transitions from the atomic ground state. The RPA oscillator strengths agree in length and velocity forms and satisfy the Thomas-Reiche-Kuhn (TRK) sum rule.[4]

Extensions of the RPA to treat allowed transitions between excited states have also been developed.[4] In these extended RPA schemes the oscillator strengths are not usually equal in velocity and length forms, and the TRK sum rule is not necessarily satisfied. It is found, however, that in the neutral-helium case the extended RPA schemes give length-form oscillator strengths which agree well with more refined calculations.

Recently we have considered a relativistic version of the RPA to treat both allowed and forbidden transitions to the atomic ground state.[5] The RRPA gives transition matrix elements which are invariant under gauge transformations and thus agree in length and velocity form, just as in the nonrelativistic version. Excited states obtained by the RRPA are intermediate coupling (IC) states in contrast to the nonrelativistic LS states. Single-photon transitions of both electric and magnetic character and of arbitrary multipolarity can be studied using RRPA; the theory provides a direct means for determining the entire complex of single-photon decays to the ground state for ions of both high and low nuclear charge Z.

In the present paper we extend the RRPA method to treat transitions between two excited states. Our generalization of the RRPA to treat excited-to-excited transitions makes use of the orbitals $w_i^{\pm}(\vec{r})$ which are the positive and negative frequency perturbations of the ground-state Dirac-Hartree-Fock (DHF) orbital $u_i(\vec{r})$ induced by an external

time-dependent potential. The perturbed orbitals satisfy a set of coupled radial Dirac equations which are solved numerically. The coupled equations are written down in Ref. 5(c) where an efficient method of solution is described.

The excited orbitals $w_i^{\pm}(\vec{r})$ are used to form a transition density matrix from which the transition matrix element can be extracted. In our numerical calculations we evaluate both DHF and RRPA oscillator strengths. The length forms of the DHF and RRPA strengths agree to better than (20%) throughout the present study; the length form of the RRPA strengths, which are presented in Sec. III, compare favorably with available precise nonrelativistic values for low Z. The velocity form of the oscillator strengths, on the other hand, are sensitive to the type of excited wave functions used and do not agree with nonrelativistic values.

As outlined in the previous discussion, the RRPA is a relativistic extension of a many-electron theory in which correlations are treated approximately. However, even for the first few elements in the He sequence, the comparisons of Sec. III show that the RRPA values agree reasonably with precise nonrelativistic calculations. For $Z>5$ the relative size of correlations is so small that the RRPA results agree accurately with the nonrelativistic values; and for high Z, the present relativistic calculations should continue to be reliable.

The $n=2$ multiplets determined by solving the RPA equations are represented by an IC scheme. In the low-Z limit these IC states reduce to LS states, while at high Z the states are described by the j-j scheme. For simplicity, we will use LS notation to designate the states when there is no possible confusion. A discussion of the $n=2$ multiplet structure as determined by solving the RRPA equations, including the transition between LS and j-j coupling, is given in Sec. IV.

III. DECAY RATES

In Fig. 1 we give energy-level diagrams for two He-like ions. The diagram for He-like Ne ($Z=10$) illustrates a low-Z situation where the states form LS multiplets; while the He-like W ($Z=74$) diagram illustrates a j-j case. As Z increases along the sequence, the $^3P_2$ state moves up close to the $^1P_1$ state; these two states become $(1s_{1/2}2p_{3/2})$ j-j states in the high-Z limit. The three states $^3P_0$, $^3P_1$, and $^1S_0$, on the other hand, stay close for all Z. Energy levels of these latter three states cross each other several times as Z increases along the sequence.

Tables and graphs are used below to describe the decays of $n=2$ states. We restrict our tables

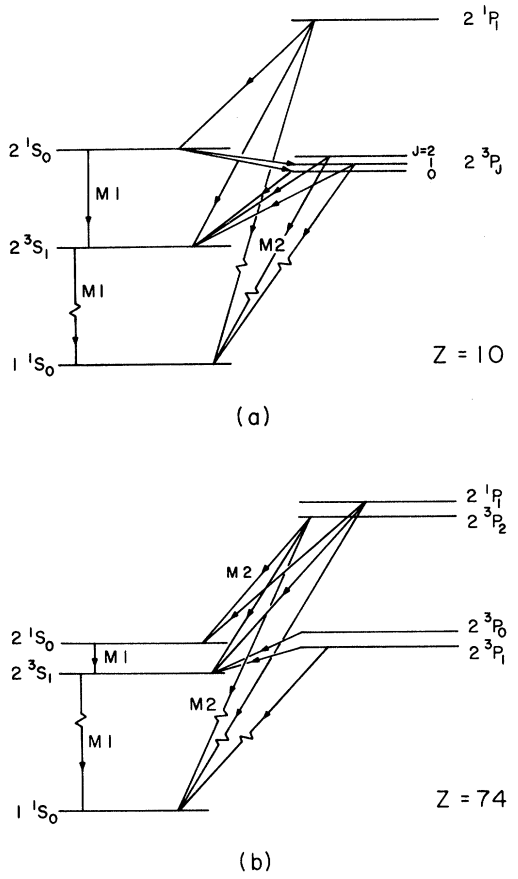

FIG. 1. Multiplet structure and various decay modes of the $n=2$ states of the helium-like (a) neon and (b) tungsten. The energy level scale is only approximate.

to $Z=2$ to 30 and selected larger values between 36 and 100.

A. $2\,^3P$ transitions

The three fine-structure components of the ^3P states decay to the ground state by entirely different modes. The $^3P_2$ state decays to the ground state by $M2$ radiation, the $^3P_1$ state decays by spin-forbidden $E1$ radiation, and the $^3P_0$ state decays by two or three photon radiation or by $E1$ radiation induced by hyperfine mixing.[6] The $2\,^3P$ states can all decay to the $2\,^3S_1$ state by allowed $E1$ radiation. The transition rate to the $2\,^3S_1$ state is small because of the small energy separation between $2\,^3P$ and $2\,^3S$; however the $E1$ transition to $2\,^3S_1$ is the dominant decay process at small Z; the competing transitions to the ground state are all highly forbidden and consequently very slow. For $Z>16$ the $2\,^3P_2$ can also decay to $2\,^1S_0$ by $M2$ radiation, but this rate remains small for all Z. There is a small range of intermediate Z for which the $2\,^3P_1$ state is above the $2\,^1S_0$ state and

for which spin-forbidden $E1$ radiation is possible; the energy separation and oscillator strength are both small for this transition so that the contribution is always insignificant.

In Table I we list the three modes of decay of the $2\,^3P_2$ state. Transitions to $2\,^3S_1$ dominate for $Z \leq 18$. At higher Z, the $M2$ decay to the ground state dominates, but the $2\,^3S_1$ channel is never insignificant.

At low Z, the $M2$ rate grows as Z^8 while the $E1$ rate grows only as Z. For larger Z however the $2\,^3P_2$ state separates from the $2\,^3S_1$ state and the $E1$ and $M2$ rates grow roughly in proportion at large Z. We also tabulate the $M2$ rate to $2\,^1S_0$ for $Z \geq 16$; this rate remains small for all Z as mentioned above.

In Table I the oscillator strengths for the $2\,^3P_2 \rightarrow 2\,^3S_1$ transition are compared with the accurate nonrelativistic calculations of Schiff *et al.*[7] for $Z \leq 10$. Except for He and Li^+, the RRPA results agree well with these precise nonrelativistic values. Thus we are confident that our results at higher Z are also reliable.

In Table II we examine the decays of the $2\,^3P_1$ state. This state can decay to the ground state by a spin-forbidden $E1$ transition or to the $2\,^3S_1$ state by a spin-allowed $E1$ transition. The decay to the $2\,^3S_1$ state is faster for $Z < 6$, but the decay to the ground state grows so rapidly that the $2\,^3S_1$ transition becomes insignificant for $Z > 12$. This be-

TABLE I. Radiative transitions from $2\,^3P_2$. Rates in sec^{-1}.

	$2\,^3P_2 \rightarrow$					
	$1\,^1S_0(M2)$	$2\,^1S_0(M2)$		$2\,^3P_2 \rightarrow 2\,^3S_1\ (E1)$		
Z	A_{RRPA}	A_{RRPA}	A_{RRPA}	A_{other} [a]	f_{RRPA}	f_{other} [b]
2	3.93(−1)		1.15(7)	1.02(7)	0.609	0.539
4	6.33(2)		3.57(7)	3.44(7)	0.223	0.213
6	2.65(4)		5.85(7)	5.72(7)	0.136	0.132
8	3.33(5)		8.31(7)	8.13(7)	0.098	0.095
10	2.27(6)		1.12(8)	1.09(8)	0.078	0.074
11	5.10(6)		1.33(8)	1.24(8)	0.071	
12	1.06(7)		1.52(8)	1.41(8)	0.066	
13	2.09(7)		1.75(8)	1.60(8)	0.061	
14	3.89(7)		2.00(8)	1.81(8)	0.058	
15	6.92(7)		2.31(8)	2.06(8)	0.055	
16	1.19(8)	4.40(−13)	2.66(8)	2.34(8)	0.053	
17	1.96(8)	1.09(−9)	3.09(8)	2.67(8)	0.051	
18	3.16(8)	3.23(−8)	3.61(8)	3.05(8)	0.050	
19	4.94(8)	3.30(−7)	4.23(8)		0.048	
20	7.55(8)	2.05(−6)	4.98(8)		0.048	
21	1.13(9)	9.44(−6)	5.90(8)		0.047	
22	1.66(9)	3.57(−5)	7.07(8)		0.047	
23	2.39(9)	1.17(−4)	8.40(8)		0.047	
24	3.39(9)	3.45(−4)	1.01(9)		0.047	
25	4.75(9)	9.31(−4)	1.22(9)		0.047	
26	6.55(9)	2.34(−3)	1.47(9)		0.047	
27	8.94(9)	5.55(−3)	1.78(9)		0.048	
28	1.20(10)	1.25(−2)	2.17(9)		0.049	
29	1.61(10)	2.70(−2)	2.64(9)		0.050	
30	2.12(10)	5.61(−2)	3.22(9)		0.050	
36	9.43(10)	2.48	1.08(10)		0.059	
42	3.33(11)	5.43(1)	3.59(10)		0.071	
45	5.85(11)	2.13(2)	6.41(10)		0.078	
50	1.38(12)	1.69(3)	1.64(11)		0.092	
56	3.50(12)	1.57(4)	4.70(11)		0.110	
65	1.19(13)	3.01(5)	2.05(12)		0.145	
74	3.47(13)	4.11(6)	7.93(12)		0.187	
80	6.62(13)	2.04(7)	1.84(13)		0.220	
100	4.31(14)	2.76(9)	2.48(14)		0.359	

[a] Dalgarno, Ref. 3.
[b] Schiff *et al.*, Ref. 7.

TABLE II. Radiative transitions from $2\,^3P_1$ and $2\,^3P_0$. Rates in $\sec^{-1}$.

	$2\,^3P_1 \rightarrow 1\,^1S_0$ ($E1$)		$2\,^3P_1 \rightarrow 2\,^3S_1$ ($E1$)			$2\,^3P_0 \rightarrow 2\,^3S_1$ ($E1$)	
Z	A_{RRPA}	f_{RRPA}	A_{RRPA}	f_{RRPA}	f_{other} [a]	A_{RRPA}	f_{RRPA}
2	2.33(2)	3.58(−8)	1.15(7)	0.608	0.539	1.15(7)	0.609
4	4.21(5)	1.96(−6)	3.57(7)	0.222	0.213	3.57(7)	0.223
6	2.89(7)	2.16(−5)	5.79(7)	0.135	0.131	5.79(7)	0.135
8	5.56(8)	1.19(−4)	8.07(7)	0.097	0.095	8.07(7)	0.097
10	5.40(9)	4.46(−4)	1.05(8)	0.077	0.074	1.04(8)	0.076
11	1.xx(10)	7.91(−4)	1.23(8)	0.069		1.21(8)	0.069
12	3.40(10)	1.30(−3)	1.37(8)	0.063		1.34(8)	0.063
13	7.62(10)	2.08(−3)	1.52(8)	0.058		1.47(8)	0.058
14	1.58(11)	3.18(−3)	1.68(8)	0.054		1.61(8)	0.054
15	3.11(11)	4.69(−3)	1.84(8)	0.051		1.75(8)	0.050
16	5.87(11)	6.77(−3)	2.02(8)	0.048		1.89(8)	0.047
17	1.04(12)	9.37(−3)	2.21(8)	0.045		2.05(8)	0.044
18	1.82(12)	1.29(−2)	2.33(8)	0.043		1.97(8)	0.041
19	3.00(12)	1.701(−2)	2.62(8)	0.041		2.38(8)	0.040
20	4.85(12)	2.22(−2)	2.84(8)	0.039		2.55(8)	0.038
21	6.98(12)	2.62(−2)	3.07(8)	0.037		2.74(8)	0.036
22	1.06(13)	3.27(−2)	3.31(8)	0.035		2.93(8)	0.035
23	1.56(13)	4.01(−2)	3.56(8)	0.034		3.14(8)	0.033
24	2.23(13)	4.82(−2)	3.80(8)	0.032		3.36(8)	0.032
25	3.12(13)	5.69(−2)	4.06(8)	0.031		3.59(8)	0.031
26	4.26(13)	6.62(−2)	4.31(8)	0.029		3.82(8)	0.030
27	5.70(13)	7.59(−2)	4.56(8)	0.028		4.08(8)	0.029
28	7.49(13)	8.57(−2)	4.82(8)	0.027		4.35(8)	0.028
29	9.65(13)	9.56(−2)	5.07(8)	0.026		4.64(8)	0.027
30	1.22(14)	0.105	5.32(8)	0.025		4.94(8)	0.027
36	3.88(14)	0.159	6.86(8)	0.020		7.18(8)	0.023
42	9.01(14)	0.194	8.50(8)	0.016		1.04(9)	0.021
45	1.28(15)	0.207	9.41(8)	0.015		1.25(9)	0.020
50	2.12(15)	0.221	1.11(9)	0.013		1.71(9)	0.019
56	3.57(15)	0.232	1.35(9)	0.012		2.49(9)	0.018
65	6.91(15)	0.238	1.83(9)	0.010		4.40(9)	0.017
74	1.21(16)	0.237	2.51(9)	0.0089		7.85(9)	0.017
80	1.68(16)	0.234	3.14(9)	0.0082		1.16(10)	0.017
100	4.27(16)	0.213	7.37(9)	0.0069		4.57(10)	0.017

[a] Schiff *et al.*, Ref. 7.

havior is due to the large energy separation $2\,^3P_1$-$1\,^1S_0$ in comparison with the $2\,^3P_1$-$2\,^3S_1$ separation. Since $A\ (\sec^{-1}) = 1.071 \times 10^{10}\omega^2 f$ with ω in a.u., we see that even though the $2\,^3P$-$1\,^1S_0$ oscillator strength is small the transition rate A is large because of the large energy separation ω.

We also list the radiative rate of $2\,^3P_0$ to $2\,^3S_1$ in Table II. This state can decay to the ground state by two-photon ($E1+M1$) or three-photon ($3E1$) processes, or (for atoms with nuclear spin $I \neq 0$) by hyperfine-induced $E1$ transitions.[6] The two- and three-photon processes have not been calculated but appear to be unimportant.[8] The transition rate $2\,^3P_0 \rightarrow 2\,^3S_1$ remains approximately equal to the $2\,^3P_1 \rightarrow 2\,^3S_1$ rate for all Z. This fact is not surprising inasmuch as the two states remain approximately degenerate from low Z (where they are part of the ^3P multiplet) to high Z (where they are part of the $1s_{1/2}2p_{1/2}$ multiplet). The oscillator strengths for the two transitions remain nearly identical throughout.

In Fig. 2 we plot the oscillator strengths of the $2\,^3P_J \rightarrow 2\,^3S_1$ transitions against Z. For the $^3P_{1,0}$ states the oscillator strengths approach zero at high Z due to the near degeneracy of $2p_{1/2}$ and $2s_{1/2}$. The $2\,^3P_2 \rightarrow 2\,^3S_1$ strength is nonzero at high Z because of the $2p_{3/2}$-$2s_{1/2}$ separation. Notice that the $^3P_2$ curve departs from the $^3P_{1,0}$ curves at $Z \approx 12$. This indicates the early deviation from nonrelativistic predictions for this transition.

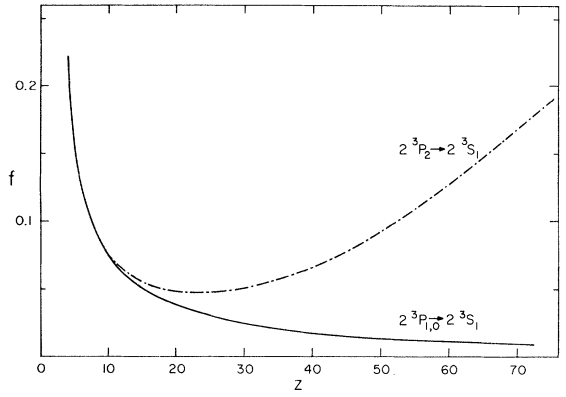

FIG. 2. Oscillator strengths of the $2\,^3P_J \rightarrow 2\,^3S_1$ ($E1$) transitions along the isoelectronic sequence. At high Z the oscillator strengths for $2\,^3P_{1,0} \rightarrow 2\,^3S_1$ transition approach zero due to the $2s_{1/2}$ and $2p_{1/2}$ degeneracy in the Dirac theory for hydrogenic systems.

B. $2\,^1P_1$ transitions

The $2\,^1P_1$ state decays primarily to the ground state by a spin-allowed $E1$ transition. We list the RRPA values of this resonance transition rate in Table III. For comparison we list the transitions to the $2\,^1S_0$ and $2\,^3S_1$ states also. These last two transitions are comparable for $Z > 30$, but they remain insignificant compared to the resonance transition. We also compare our computed oscillator strengths for the $2\,^1P_1 \rightarrow 2\,^1S_0$ transition with the values of Schiff *et al.* for $Z \leq 10$, obtaining good agreement.

C. $2\,^1S_0$ transitions

In Table IV, we list the transition modes from the $2\,^1S_0$ state. This state decays principally by a two-photon ($2E1$) transition to the ground state.[3] The $2E1$ rates are much larger than the competing

TABLE III. Radiative transitions from $2\,^1P_1$. Rates in sec^{-1}.

	$2\,^1P_1 \rightarrow 1\,^1S_0$ ($E1$)		$2\,^1P_1 \rightarrow 2\,^1S_0$ ($E1$)			$2\,^1P_1 \rightarrow 2\,^3S_1$ ($E1$)	
Z	A_{RRPA}	f_{RRPA}	A_{RRPA}	f_{RRPA}	f_{other}[a]	A_{RRPA}	f_{RRPA}
2	1.71(9)	0.252	1.93(6)	0.392	0.376	1.29(0)	0.157(−7)
4	1.21(11)	0.544	9.49(6)	0.156	0.149	3.65(2)	0.752(−6)
6	8.86(11)	0.644	1.79(7)	0.097	0.093	7.69(3)	0.564(−5)
8	3.30(12)	0.692	2.69(7)	0.071	0.068	6.37(4)	0.235(−4)
10	8.85(12)	0.719	3.71(7)	0.056	0.053	3.24(5)	0.710(−4)
11	1.34(13)	0.729	4.29(7)	0.051		6.49(5)	0.114(−3)
12	1.95(13)	0.736	4.93(7)	0.047		1.22(6)	0.175(−3)
13	2.74(13)	0.742	5.66(7)	0.044		2.19(6)	0.259(−3)
14	3.76(13)	0.746	6.49(7)	0.041		3.76(6)	0.372(−3)
15	5.03(13)	0.749	7.47(7)	0.039		6.22(6)	0.519(−3)
16	6.59(13)	0.751	8.61(7)	0.037		9.96(6)	0.707(−3)
17	8.47(13)	0.752	9.97(7)	0.036		1.55(7)	0.942(−3)
18	1.07(14)	0.753	1.16(8)	0.035		2.36(7)	0.123(−2)
19	1.34(14)	0.750	1.36(8)	0.034		3.50(7)	0.157(−2)
20	1.65(14)	0.747	1.61(8)	0.033		5.10(7)	0.198(−2)
21	2.00(14)	0.743	1.91(8)	0.032		7.28(7)	0.244(−2)
22	2.41(14)	0.737	2.28(8)	0.032		1.02(8)	0.297(−2)
23	2.87(14)	0.731	2.74(8)	0.032		1.41(8)	0.356(−2)
24	3.38(14)	0.723	3.32(8)	0.032		1.93(8)	0.421(−2)
25	3.96(14)	0.715	4.05(8)	0.032		2.60(8)	0.490(−2)
26	4.59(14)	0.706	4.96(8)	0.032		3.46(8)	0.564(−2)
27	5.29(14)	0.697	6.10(8)	0.032		4.56(8)	0.642(−2)
28	6.06(14)	0.687	7.53(8)	0.032		5.95(8)	0.724(−2)
29	6.90(14)	0.676	9.33(8)	0.033		7.70(8)	0.808(−2)
30	7.81(14)	0.666	1.16(9)	0.033		9.89(8)	0.894(−2)
36	1.51(15)	0.608	4.36(9)	0.038		3.93(9)	0.0143
42	2.66(15)	0.563	1.60(10)	0.045		1.36(10)	0.0201
45	3.43(15)	0.544	2.98(10)	0.050		2.43(10)	0.0232
50	5.08(15)	0.517	8.03(10)	0.058		6.14(10)	0.0286
56	7.79(15)	0.490	2.45(11)	0.071		1.75(11)	0.0358
65	1.37(16)	0.454	1.13(12)	0.093		7.47(11)	0.0483
74	2.24(16)	0.418	4.53(12)	0.121		2.84(12)	0.0630
80	3.01(16)	0.394	1.07(13)	0.142		6.53(12)	0.0742
100	6.79(16)	0.303	1.49(14)	0.232		8.53(13)	0.121

[a] Schiff *et al.*, Ref. 7.

$M1$ rate to the $2\,^3S_1$ state.

The $2\,^1S_0$ state can also decay to the $2\,^3P_1$ state by a spin-forbidden $E1$ transition in the ranges of Z for which the $2\,^1S_0$ lies higher in energy. Since the $2\,^1S_0$ and $2\,^3P_1$ states are always close in energy and since the oscillator strength is small, this transition never competes effectively with the $2E1$ decay.

The RRPA calculation of the $M1$ rate given in Table IV involves substantial numerical cancellation and is probably only accurate to within a factor of 2.

D. $2\,^3S_1$ transitions

The $2\,^3S_1$ state is lowest in energy among the $n=2$ multiplets. The state can decay to the ground state by a single-photon $M1$ transition or by a two-photon ($2E1$) process. In Table V we list both rates along the isoelectronic sequence. The decay is dominated by the $M1$ transition for all Z.

IV. EXCITATION ENERGIES

It has been mentioned that the energy pattern of the $n=2$ states varies considerably along the isoelectronic sequence. Since the transition rates and directions are sensitive functions of the energy separations, we consider here the RRPA predictions for the multiplet splittings. The purpose of the present discussion is twofold: first, to show that the RRPA predicts the $n=2$ multiplet structure with sufficient accuracy to give reliable decay

TABLE IV. Radiative transitions from $2\,^1S_0$. Rates in sec^{-1}.

Z	$2\,^1S_0 \rightarrow 2\,^3S_1$ ($M1$) A_{RRPA}	$2\,^1S_0 \rightarrow 2\,^3P_1$ ($E1$) A_{RRPA}	$2\,^1S_0 \rightarrow 1\,^1S_0$ ($2E1$) A_{other} [a]
2	1.51(−7)		5.13(1)
4	7.96(−5)		1.81(4)
6	1.95(−3)		3.31(5)
8	1.73(−2)	1.15(0)	2.31(6)
10	9.15(−2)	2.08(1)	1.00(7)
11	1.85(−1)	3.65(2)	1.85(7)
12	3.52(−1)	6.50(2)	3.22(7)
13	6.33(−1)	1.06(3)	5.34(7)
14	1.09(0)	1.60(3)	8.47(7)
15	1.81(0)	2.23(3)	1.31(8)
16	2.90(0)	2.90(3)	1.96(8)
17	4.51(0)	3.51(3)	2.83(8)
18	6.86(0)	3.96(3)	4.04(8)
19	1.02(1)	4.16(3)	
20	1.48(1)	4.05(3)	
21	2.12(1)	3.63(3)	
22	2.98(1)	2.98(3)	
23	4.13(1)	2.20(3)	
24	5.65(1)	1.43(3)	
25	7.63(1)	7.95(2)	
26		3.46(2)	
27	1.35(2)	9.93(1)	
28	1.76(2)	1.03(1)	
29	2.29(2)		
30	2.95(2)		
36	1.16(3)		
42	3.78(3)		
45	6.48(3)		
50	1.50(4)	1.56(2)	
56	3.80(4)	2.54(4)	
65	1.37(5)	5.35(5)	
74	4.50(5)	3.48(6)	
80	9.70(5)	9.15(6)	
100	1.24(7)	1.08(8)	

[a] Dalgarno, Ref. 3.

TABLE V. Radiative transitions from $2\,^3S_1$. Rates in sec^{-1}.

Z	$2\,^3S_1 \rightarrow 1\,^1S_0$ ($M1$) A_{RRPA}	$2\,^3S_1 \rightarrow 1\,^1S_0$ ($2E1$) A_{other} [a]
2	1.73(−4)	4.02(−9)
4	5.91(−1)	6.36(−5)
6	4.96(1)	8.93(−3)
8	1.06(3)	2.54(−1)
10	1.10(4)	3.20(0)
11	2.97(4)	
12	7.33(4)	
13	1.68(5)	
14	3.61(5)	
15	7.36(5)	
16	1.43(6)	
17	2.67(6)	
18	4.80(6)	
19	8.37(6)	
20	1.42(7)	
21	2.33(7)	
22	3.76(7)	
23	5.93(7)	
24	9.17(7)	
25	1.39(8)	
26	2.08(8)	
27	3.06(8)	
28	4.45(8)	
29	6.37(8)	
30	9.01(8)	
36	5.85(9)	
42	2.86(10)	
45	5.82(10)	
50	1.74(11)	
56	5.66(11)	
65	2.73(12)	
74	1.10(13)	
80	2.58(13)	
100	3.29(14)	

[a] Dalgarno, Ref. 3.

rates; and second, to give some new results for the multiplet structure in the high Z region ($Z > 30$) where only limited alternative calculations exist.

A. Fine-structure splittings of the $2\,^3P$ states

The fine structure of the $2\,^3P$ states in the He sequence provides an interesting situation where the Landé interval rule is not followed. Accurate calculations by Accad *et al.*[9] show that the energies E_J of the $2\,^3P_J$ states follow the ordering $E_0 > E_1 > E_2$ in He and $E_0 > E_2 > E_1$ in Li^+. For Be^{2+}, B^{3+}, and C^{4+} the ordering is $E_2 > E_0 > E_1$. Beginning with N^{5+} nonrelativistic calculations[10] using the Pauli approximation to account for relativistic effects predict the ordering $E_2 > E_1 > E_0$. The present calculations agree with the accurate nonrelativistic predictions for low and intermediate Z. However, at high Z ($Z \gtrsim 45$), we show that the ordering changes to $E_2 > E_0 > E_1$.

In Fig. 3 we plot the ratio $R = (E_1 - E_0)/(E_2 - E_1)$ along the sequence. This ratio peaks at $Z \cong 15$ in agreement with the calculation of Ermolaev and Jones[10]; for large Z the ratio becomes negative, in agreement with the relativistic $1/Z$ calculations of Doyle.[11]

The fact that $E_0 > E_1$ at high Z is not difficult to understand. At high Z, both $^3P_1$ and $^3P_0$ belong to the $(1s_{1/2}2p_{1/2})$ multiplet, but $^3P_1$ has a small admixture of $(1s_{1/2}2p_{3/2})$ whereas $^3P_0$ is a pure state. On the other hand, $^1P_1$ and $^3P_2$ both belong to $(1s_{1/2}2p_{3/2})$ at high Z; $^3P_2$ is a pure state while $^1P_1$ contains a small admixture of $1s_{1/2}2p_{1/2}$. In accordance with the familiar "spectral repulsion" rule, the small impurities in $^3P_1$ and $^1P_1$ result in the shift of energy away from the pure states

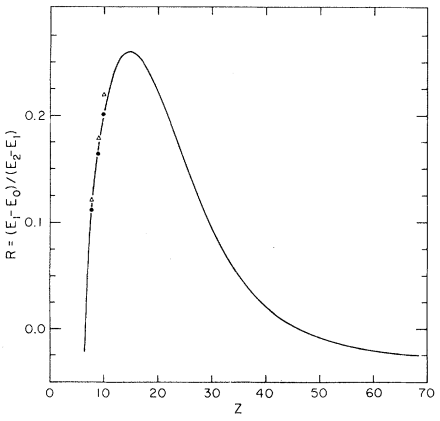

FIG. 3. Energy-level separations among the $2\,^3P_J$ states. The curve is a plot of $R = (E_1 - E_0)/(E_2 - E_1)$ where E_J is the energy of $2\,^3P_J$. The triangles at $Z = 8$, 9, 10 are the results of Accad *et al.* (Ref. 9), and the dots are the presents results.

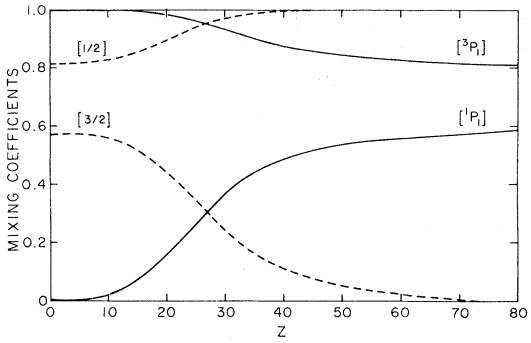

FIG. 4. Mixing coefficients of the physical $^3P_1$ state in terms of LS states $[^3P_1]$ and $[^1P_1]$ are plotted against Z using solid lines. The j-j mixing coefficients of $^3P_1$ are plotted using dashed lines.

$^3P_0$ and $^3P_2$ by increasing their separation. Thus at high Z, $^1P_1$ lies higher than $^3P_2$ and $^3P_1$ lies lower than $^3P_0$.

To see how the admixture of pure states varies with Z, we plot in Fig. 4 the magnitude of the mixing coefficients for the $^3P_1$ state in terms of LS states designated by $[^1P_1]$ and $[^3P_1]$ and of j-j states. Notice the fast rise of the $[^1P_1]$ component for $Z \geq 20$. For $Z > 30$, the spin-forbidden and spin-allowed $E1$ transition terminology is meaningless because of the large mixing. The $(1s_{1/2}2p_{3/2})$ component of $^3P_1$ dies out slowly as Z increases.

B. Relative positions of $n = 2$ sates

Among the $n = 2$ states, the $^1P_1$ state is always highest in energy and the $^3S_1$ is always lowest. The positions of the other four states $^3P_{0,1,2}$ and $^1S_0$ vary along the isoelectronic sequence. For higher Z, $^3P_2$ approaches $^1P_1$ and is well separated from the other three. These three states $^3P_{0,1}$

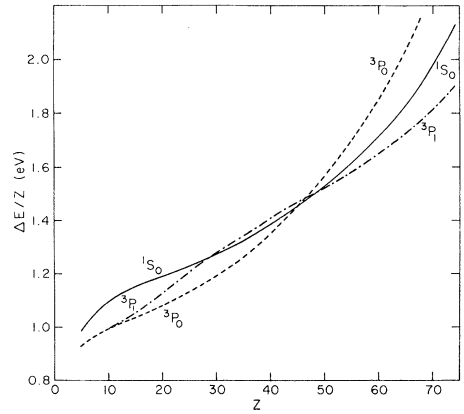

FIG. 5. Energy differences of the three states $^3P_0$, $^3P_1$, and $^1S_0$ with respect to ^3S are plotted against Z.

and $^1S_0$ remain close for all Z and change relative positions frequently. In Fig. 5 we plot $[E^{(x)} - E(^3S_1)]/Z$ in eV for the three levels $x = {}^1S_0$, $^3P_1$, $^3P_0$. The relative positions of $^3P_1$ and $^3P_0$ have been discussed above. Notice that the $^1S_0$ position lies below $^3P_1$ only within a limited region of Z; the transition $2\,{}^1S_0 \rightarrow 2\,{}^3P_1$ is impossible in this limited region.

---

*Work supported in part by ERDA Contract No. E(11-1)-2887.

† Work supported in part by NSF Grant No. GP-42738.
Permanent address: Dept. of Physics, Notre Dame University, Notre Dame, Ind. 46656.

[1]A. H. Gabriel and C. Jordan, Case Stud. At. Phys. 2, 211 (1972).

[2]I. Martinson and A. Gaupp, Phys. Rep. 15C, 115 (1974).

[3]A. Dalgarno, *The Menzel Symposium,* NBS Spec. Publ. No. 353 (U.S. GPO, Washington, D. C., 1971), p. 47.

[4]M. Ya. Amusia and N. A. Cherepkov; Case Stud. At. Phys. 5, 47 (1975); T. N. Chang and U. Fano, Phys. Rev. A 13, 263 (1976); D. L. Yeager, M. A. C. Nacimento, and V. McKoy, Phys. Rev. A 11, 1168 (1975); Gy. Csanak, J. Phys. B 7, 1289 (1974).

[5](a) W. R. Johnson and A. Dalgarno (unpublished); (b) W. R. Johnson, C. D. Lin, and A. Dalgarno, J. Phys. B 9, L303 (1976); (c) W. R. Johnson and C. D. Lin, Phys. Rev. A 14, 565 (1976).

[6]P. J. Mohr, in *Proceedings of the Fourth International Conference on Beam-Foil Spectroscopy and Heavy-Ion Atomic Physics, Gatlinburg, Tenn.*, 1975 (Plenum, New York, 1976).

[7]B. Schiff, C.L. Pekeris, and Y. Accad, Phys. Rev. A 4, 885 (1971).

[8]The two-photon ($E1+M1$) decay of $2\,{}^3P_0$ to the ground state should be smaller than the two-photon ($2E1$) decay of $2\,{}^1S_0$ by a factor R^2, where R is roughly the ratio of atomic size to the characteristic transition wavelength. From the two-photon decay rates of $2\,{}^1S_0$ given in Table IV, we expect the two-photon process in $2\,{}^3P_0$ to be insignificant compared with the $2\,{}^3P_0 \rightarrow 2\,{}^3S_1$ ($E1$) transition.

[9]Y. Accad. C. L. Pekeris, and B. Schiff, Phys. Rev. A 4, 516 (1971).

[10]A. M. Ermolaev and M. Jones, J. Phys. B 7, 199 (1974).

[11]H. Doyle, Adv. At. Mol. Phys. 5, 337 (1969).